Proceedings Paper:

Han, Yaofei, Gong, Chao, Zhao, Xing orcid.org/0000-0003-4000-0446 et al. (1 more author) (2023) MPC-based Coordination Control of Dual DirectDrive Permanent Magnet Motors Used in Coal Mining Belt Conveyors. In: IECON 2023-49th Annual Conference of the IEEE Industrial Electronics Society. IECON 2023- 49th Annual Conference of the IEEE Industrial Electronics Society, 16-19 Oct 2023 IEEE , SGP

https://doi.org/10.1109/IECON51785.2023.10311946

MPC-based Coordination Control of Dual Direct-Drive Permanent Magnet Motors Used in Coal Mining Belt Conveyors

Yaofei Han
National Maglev Transportation Engineering R&D Center
Tongji University
Shanghai, China
hanyaofei@126.com

Chao Gong
Department of Electrical and Computer Engineering
University of Alberta
Edmonton, Canada
gongchaonpu@gmail.com

Shaofeng Chen
National Maglev Transportation Engineering R&D Center
Tongji University
Shanghai, China
chenshaofeng@tongji.edu.cn

Zhixun Ma
National Maglev Transportation Engineering R&D Center
Tongji University
Shanghai, China
zhixun.ma@tongji.edu.cn

Xing Zhao
School of Physics, Engineering and Technology
University of York
York, the UK
xing.zhao@york.ac.uk

IECON 2023- 49th Annual Conference of the IEEE Industrial Electronics Society | 979-8-3503-3182-0/23/$31.00 ©2023 IEEE | DOI: 10.1109/IECON51785.2023.10311946

***Abstract*— In the application of coal mining belt conveyors, dual-motor drives based on permanent magnet motors (PMM) are gaining increasing attention now. To achieve high-performance coordination control of the two motors, this paper proposes a finite control set model predictive speed control (FCS-MPSC) method to improve the dynamics and speed tracking performance of the motors. First, the features of the dual-motor drives used in conveyor belts are analyzed. On this basis, the requirements of the control strategies are illustrated. Second, a master-slave control strategy is developed after treating the PMMs at the tail end and head end as the master motor and slave motor, respectively. Third, the FCS-MPSC method is developed for both master and slave motors by using new predicting model. In this process, the issue that the speed property is not directly related to the manipulated variables are tackled. Moreover, in order to further improve the dynamics of the slave motor, a speed reference compensation strategy is proposed. Finally, the proposed FCS-MPSC method is validated through comparative simulation results.**

***Keywords*— permanent magnet motor, coordination control, model predictive control, belt conveyor, dual motors**

I. INTRODUCTION

The traditional drive system employed in coal mine conveyor belts comprises a solitary asynchronous motor and gears to generate power [1]. This configuration exhibits several characteristics. First, the single motor necessitates a substantial power capacity without possessing redundancy [2]. Hence, in the event of motor failure, there exists no backup equipment to supply power. Second, the utilization of gear structures induces wear and escalates maintenance expenses [3]. Third, asynchronous motors typically employ variable frequency control methods grounded on the voltage-to-frequency (V/F) concept, which results in suboptimal overall energy efficiency and an incapacity to meet the demands of contemporary high-efficiency systems [4]. On these grounds, the conveyor belt system driven by dual direct-drive permanent magnet motors (PMMs), as depicted in Fig. 1, has garnered growing attention [5-9]. This system primarily comprises the subsequent components. 1) Belt: Conveyor belt constitutes a continuous loop composed of diverse layers of rubber or fabric material. Its principal function entails transporting coal and furnishing the requisite strength to accommodate the load. Conveyor belts employed in coal mining operations are typically designed to possess sturdiness

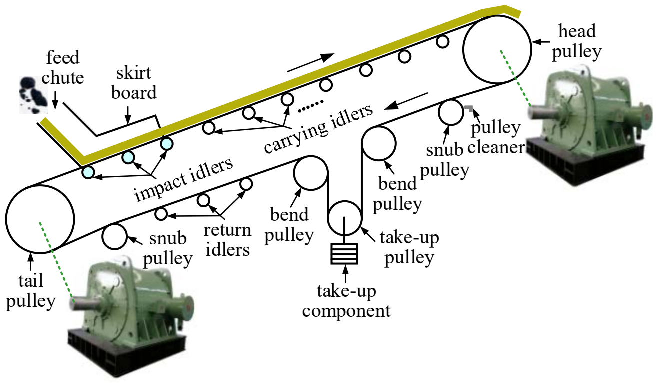

Fig. 1 Diagram of dual-PMM-based coal mining belt conveyor

and resistance to abrasion, as coal can exhibit abrasive properties. 2) Pulleys: Pulleys represent cylindrical devices deployed to alter the direction of the belt or provide tension. The head pulley occupies the discharge end of the conveyor and assumes the responsibility of driving the belt. Correspondingly, the tail pulley situated at the loading end also imparts driving force. Additionally, bend pulleys serve the purpose of maintaining the proper alignment and tension of the conveyor belt as it changes direction around curves or bends. 3) Dual-motor drive system: This system encompasses a pair of direct-drive permanent magnet motors directly linked to the head and tail pulleys. The motors may possess identical or distinct power ratings. 4) Idlers: Idlers denote support rollers positioned along the conveyor's length to uphold the belt and sustain its alignment. They diminish friction and facilitate the smooth movement of the belt. Certain idlers are designed to furnish supplementary support and mitigate sagging. 5) Take-up system: The take-up system assumes the responsibility of preserving tension in the conveyor belt to avert slippage. Typically, it comprises a take-up pulley, a gravity take-up mechanism, and a counterweight. 6) Cleaning system: The cleaning system functions to eliminate residual coal deposits from the belt and pulleys, thereby mitigating complications such as belt jamming and operational vibrations. 7) Load zone: The load zone designates the region wherein coal is loaded onto the conveyor belt. Frequently, this zone incorporates elements such as chutes, skirting boards, and impact idlers to regulate the impact and confine the material being loaded. Compared to the traditional coal mine conveyor belt drive system, the new system exhibits high efficiency and high reliability.

In terms of the dual-PMM-based coal mining belt conveyor, in order to achieve higher efficiency, the drive algorithm is not limited to V/F control [10], [11]. Among them, speed and current closed-loop control have promising applications. However, the conveyor belt used for coal mining presents challenges to closed-loop control [12]. Specifically, because the two motors are connected through the belt, their speeds need to be consistent to achieve coordination control [13], [14]. However, for the motor connected to the tail pulley, it is closer to the loading position where coal is loaded, resulting in more severe external disturbances and greater speed fluctuations. Comparatively, the motor connected to the head pulley suffers relatively smaller external disturbances, and its own speed variation range is smaller as well. However, the speed differences between the two motors in a dual-PMM-based coal mining belt conveyor can lead to several issues with the belt. 1) Belt misalignment: If the speeds of the two motors are significantly different over time, it can cause the belt to deviate from its intended path. This misalignment can result in uneven loading, increased friction, and potential damage to the belt and other conveyor components. 2) Uneven tension distribution: Speed variations between the motors can lead to inconsistent tension distribution along the belt. This can result in areas of the belt being under excessive tension, leading to premature wear and potential failure. These two aspects can accelerate wear and tear on the belt, leading to increased maintenance and replacement costs. It may also require more frequent adjustments and alignments to ensure proper functioning of the conveyor system. 3) Reduced conveying capacity: Inefficient coordination between the two motors can lead to a decrease in overall conveying capacity. The uneven distribution of power and tension can casue decreased productivity. Hence, it is significant to develops effective strategies that can guarantee coordination control.

This paper proposes an MPC-based coordination control strategy to regulate the speeds of two PMMs used in caol mining belt conveyors. The main contributions of the paper are as follows:

1) The PMMs connected with the tail pulley and head pulley are defined as master and slave motors, respectively. Considering that the master motor experiences more obvious speed variations, the slave motor needs to follow the real speed of the master motor.

2) A model predictive control (MPC)-based coordination control strategy is developed. The rationale behind this method is that high dynamics contribute to synchronous operations, which is clearly explained in this paper.

3) To achive satisfying dynamic performance, a model predictive speed controller (MPSC) is proposed. When desining the MPSC, the issue that manpulated voltages are not directly related to the motor speed property is tackled. Simulation results prove that the proposed method can achieve good coordination control performance.

II. Modeling of PMM

In the forthcoming analysis and design of control algorithms, the motor model serves as a fundamental prerequisite. Hence, this section presents the mathematical model of the permanent magnet motor to establish a basis for subsequent investigations. The commonly used state-space model that describes both electrical and mechanical properties of PMMs can be written as follows [15]:

$$\frac{\mathrm{d}i_d}{\mathrm{d}t} = -\frac{R_s}{L_d} i_d + \frac{L_q}{L_d} p\omega_m i_q + \frac{u_d}{L_d} \tag{1}$$

$$\frac{\mathrm{d}i_q}{\mathrm{d}t} = -\frac{L_d}{L_q} p\omega_m i_d - \frac{R_s}{L_q} i_q + \frac{u_q}{L_q} - \frac{\Psi_f}{L_q} p\omega_m \tag{2}$$

$$T_e = 1.5p(\Psi_f i_q + (L_d - L_q) i_d i_q) \tag{3}$$

$$\frac{\mathrm{d}\omega_m}{\mathrm{d}t} = \frac{1}{J}(1.5p(\Psi_f i_q + (L_d - L_q) i_d i_q) - B\omega_m - T_l) \tag{4}$$

where i_d, i_q are d, q-axis currents. u_d, u_q are d, q-axis voltages. L_d, L_q are d, q-axis inductances. R_s is stator resistance. p is the number of pole pairs. T_e, T_l and ω_m are electromagnetic torque, load torque, and rotor speed, respectively. Ψ_f is permanent magnet flux linkage. J and B are rotor inertia and viscous coefficient, respectively.

III. Proposed MPC-based Coordination Control Method

A. Rationale of Control Strategy Design

In the context of driving conveyor belts, achieving consistent rotational speeds of the two motors involved is the ultimate objective. Several methods can be employed to ensure speed coordination. The first approach is the independent control method [16]. In this method, both motors have a reference speed set to the target speed, resulting in no interactions or intercommunication between the motors. However, when the motor located at the tail end experiences external disturbances, the motor at the head end fails to respond promptly, leading to speed deviations. The second commonly used method is the master-slave control strategy [17]. One of the two motors is designated as the master motor, while the other operates as the slave motor. The reference speed of the master motor is set to the target speed, while the reference speed of the slave motor is determined based on the real-time speed of the master motor. This method couples the operation of both motors, and as long as the slave motor possesses excellent dynamic tracking capabilities, the speed coordination between the two motors can be achieved. The third method is the coupled control method [18]. It involves calculating the speed error between the two motors. For the motor with a lower speed, the error is added proportionally to the reference speed, while for the motor with a higher speed, the error is subtracted proportionally from the reference speed. This method yields effective control performance for steady-state operation of the two motors. However, for the conveyor belt's driving motors, the speed differences primarily arise from external disturbances. Even by adjusting the real-time reference speed, the motor located closer to the tail end cannot stabilize at the new reference speed due to disturbances. Therefore, the coordination control method provided by this approach remains unsatisfactory. In summary, the master-slave control method exhibits superiority in conveyor belt applications. Considering practical operating conditions, the motor positioned at the tail end, which is more susceptible to disturbances, is defined as the master motor, while the motor at the head end is defined as the slave motor.

For the PMM (master motor) connected to the tail pulley, which is more vulnerable to external disturbances, it is crucial to ensure the motor's robustness. Specifically, the motor

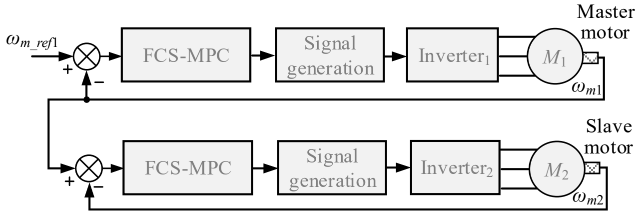

Fig. 2. Speed coupling strategy used for coordination control.

should exhibit minimal speed fluctuations when subjected to load disturbances and should quickly recover from speed deviations. Taking the traditional PI-based field-oriented dual-closed-loop control as an example, when a speed deviation occurs, the PI output of the speed loop automatically adjusts to restore the speed to the reference value. However, due to integral delay, the adjustment time tends to be relatively long. Therefore, for motors used in conveyor belt drives, control algorithms that offer high-speed tracking response and dynamic response need to be developed. Currently, finite control set (FCS) model predictive control (MPC) methods based on optimal control theory have shown promise [19].

As for the motor (slave motor) connected to the head pulley, it is essential to possess a high dynamic response to track the real-time speed of the master motor. The motor's response speed depends on the rotor inertia and the control algorithm. In practical scenarios, for motors with fixed rotor inertia, increasing the control system's bandwidth can achieve high dynamic response [20]. In this regard, the FCS-MPC algorithm is a suitable choice to meet the requirement.

B. Speed Coupling Between Two PMMs

Fig. 2 shows the speed coupling strategy employed for coordination control. It needs to be addressed that the master motor is the one connected with the tail pulley, and the slave motor is the one connected with the head pulley. ω_{m_ref1} is the desired motor speed, working as the reference of the master motor. ω_{m1} is the real speed of the master motor, serving as the reference of the slave motor. ω_{m2} is the real speed of the slave motor, which needs to track the speed of the master motor.

C. Proposed MPSC

In Fig. 2, for each motor, only one FCS-MPC controller is adopted to regulate the motor speed. In this case, only one control loop is included. This approach focuses solely on achieving the desired motor speed without the need for a current regulator. It maximizes the system bandwidth and enhances the dynamic response speed. Now, a new issue how to design the FCS-MPSC controller arises.

a) Design of MPC for both master and slave motors

Because speed is the target objective to be regulated, the future speed information needs to be predicted. Traditionally, forward Euler algorithm should be applied to the machine model for future state estimation. However, this method is not suitable for a PMM. In detail, the forward Euler discretization algorithm cannot be applied to (4). This happens because there is no voltage information which represents the control variable in (4). To solve this issue, by carefully looking at (4), it can be seen that speed is a direct consequence of the currents in each control period, and integral can make this relationship more pronounced. Take definite integral of (4) between t_k and t_{k+1} and the predicting model for speed estimation is [21], [22]:

$$\omega_m(k+1) = \frac{1.5p\Psi_f}{J}\int_{t_k}^{t_{k+1}} i_q \mathrm{d}t + \frac{L_d - L_q}{J}\int_{t_k}^{t_{k+1}} i_d i_q \mathrm{d}t - \frac{1}{J}\int_{t_k}^{t_{k+1}} T_l \mathrm{d}t + \omega_m(k) \tag{5}$$

where $\omega_m(k)$ and $\omega_m(k+1)$ are current and future speed information, respectively. $T_l(k)$ is load. In practice, the control period T is short, so an appropriate assumption that i_q and $i_d i_q$ will witness linear changes within a control period, and the external load torque T_l remains constant over the period can be made. In this case, (5) can be rewritten as:

$$\omega_m(k+1) = \frac{3p\Psi_f T}{4J}(i_q(k+1) - i_q(k)) - \frac{T_l(k)T}{J} + \omega_m(k) + \frac{(L_d - L_q)T}{2J}(i_d i_q(k+1) - i_d i_q(k)) \tag{6}$$

From (6), it can be noticed that before predicting the future speed, the future currents and load should be calculated. As for the future currents, after applying Euler discretization algorithm to (1) and (2), the predicting model can be obtained as:

$$i_d(k+1) = \frac{L_d - TR_s}{L_d} i_d(k) + \frac{TL_q p}{L_d}\omega_m(k) i_q(k) + \frac{T}{L_d} u_d(k) \tag{7}$$

$$i_q(k+1) = -\frac{TL_d p}{L_q}\omega_m(k) i_d(k) + \frac{L_q - TR_s}{L_q} i_q(k) + \frac{T}{L_q} u_q(k) - \frac{T\Psi_f p}{L_q}\omega_m(k) \tag{8}$$

where $i_d(k)$ and $i_q(k)$ are the measured current information at t_k. $i_d(k+1)$ and $i_q(k+1)$ are the future currents at t_{k+1}. In terms of the load, it can be assumed to equal the electromagnetic torque, which can be derived from (3) as:

$$T_l(k) = 1.5p(\Psi_f i_q(k) + (L_d - L_q) i_d(k) i_q(k)) \tag{9}$$

Relying on the predicting model (5) ~ (9), the future speed information $\omega_m(k+1)$ can be calculated at t_k. And the implementation procedures can be further summarized as:

a) Measurement: Measure the phase currents rotor speed $\omega_m(k)$ and position $\theta(k)$ by the use of physical sensors.

b) Coordinate transformation: Transform phase currents into the *d*, *q*-axis currents $i_d(k)$ and $i_q(k)$ relying on the position information $\theta(k)$.

c) Current and torque information calculation: Employ the discrete model (7) ~ (9) to predict the future currents $i_d(k+1)$ and $i_q(k+1)$ and the real-time load $T_l(k)$ for seven candidate voltage vectors.

d) Speed prediction: Use the discrete model (5) to predict the future speed $\omega_m(k+1)$ corresponding to different voltage vectors.

e) Evaluation and switching state selection: Substitute the predicted speed into the cost function (10) one by one to select the voltage vector minimizing the cost function.

$$g_i = (\omega_m^* - \omega_m(k+1))^2 \tag{10}$$

where ω_m^* is reference speed.

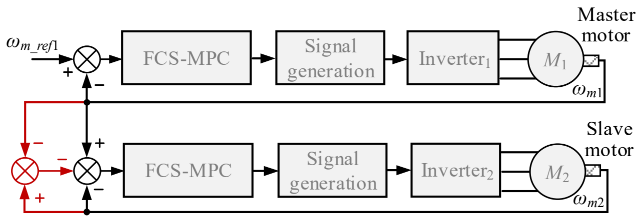

Fig. 3. Modified control scheme used for conveyor belt.

f) Actuation: Apply the optimal switching state associated with the optimal voltage vector selected in *e*) to the inverter.

b) Reference speed compensation for slave motor

The proposed FCS-MPSC has high dynamics. In theory, the slave motor can keep in pace with master motor's speed. However, the dynamics of the slave motor can be further improved by incorporating the speed errors between the two motors into the control process. Fig. 3 shows the modified control scheme, in which the reference speed of the slave motor is set as:

$$\begin{cases} \omega_{m\_ref2} = \omega_{m1}, \; if \;\; \omega_{m1} = \omega_{m2} \\ \omega_{m\_ref2} = 2\omega_{m1} - \omega_{m2}, \; if \;\; \omega_{m1} \neq \omega_{m2} \end{cases} \tag{11}$$

where ω_{m_ref2} is reference speed of the slave motor.

IV. Verification Results

In order to verify that the proposed FCS-MPSC-based coordination method can show good performance, simulation is conducted on a dual-PMM drive whose motor parameters are presented in Table I. The system model used for simulation is established in MATLAB/ Simulink 2018b, which is shown in Fig. 4 [23].

To verify the effectiveness of the proposed MPC-based coordination control strategy, simulation is conducted on the motor under the speed of 40 rad/s and under the load of 60 Nm. Fig. 5 shows the simulation results of speed, torque, and currents. First, the speed can reach and stabilizes at the desired level for both the master and slave motors. Second, at the start-up stage, because the motor rotates under a heavy load, the motor speed becomes negative for a short while. Third, As for the slave motor, it can track the speed of the master speed precisely at the stable state, while it cannot track the speed of the master speed at the start-up stage. This needs to be further improved in the future.

To verify that when two motors work under stable states, the tracking performance of slave motor is good when master motor's speed fluctuates, the following setups are given. When two motors rotate at 40 rad/s under the load of 60 Nm, the master motor experiences sinewave speed fluctuations by changing the reference speed. The simulation results are shown in Fig. 6. It can be seen that the slave motor is inclined

TABLE I
MOTOR AND CONTROL PARAMETERS

Parameter	Value	Unit
stator winding resistance R_s	0.6383	Ω
d-axis inductance L_d	2	mH
q-axis inductance L_q	2	mH
the number of pole pairs *p*	4	-
DC-bus voltage U_{dc}	530	V
flux linkage Ψ_f	0.085	Wb
rated motor speed ω_m	40	rad/s
sampling time *T*	0.1	ms

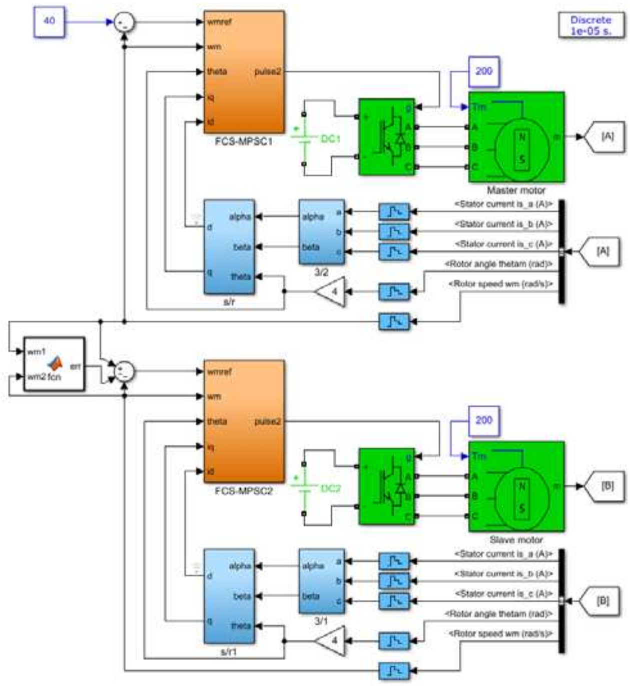

Fig. 4. Simulation model used for verifying proposed strategies.

to track the master motor's working status, though they are not totally the same. This means that the proposed method has relatively high coordination control performance, which requires further improvement in the future.

Fig. 7 shows the performance of master and slave motors when the load of master motor fluctuates, which complies with the real applications. First of all, it can be seen that when load variations exist, the motor speed fluctuates. Second, similar to Fig. 6, the slave motor speed relatively tracks the master motor speed, proving that further exploration is required.

V. Conclusion

To achieve coordination control of double PMMs used to actuate coal mining belt conveyors, this paper develops a master-slave control strategy and FCS-MPSC controller. First, the working mechanism of the dual PMMs in the application of coal mining belt conveyors is explained. It can be found that the PMM located at the tail end is inclined to experience higher external disturbances than the motor at the head end.

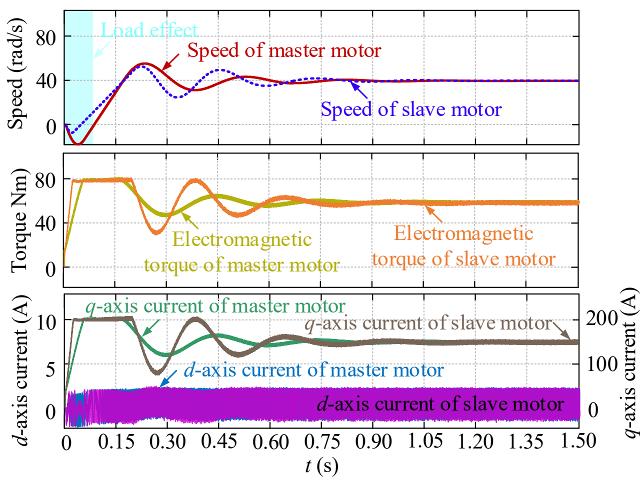

Fig. 5. Effectiveness of proposed strategies.

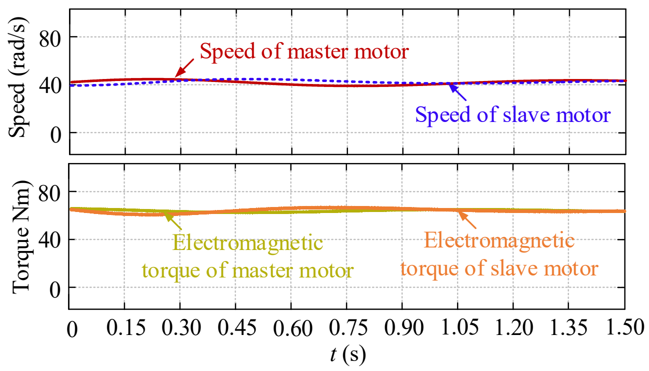

Fig. 6. Simulation results when master motor experiences sinewave speed fluctuations.

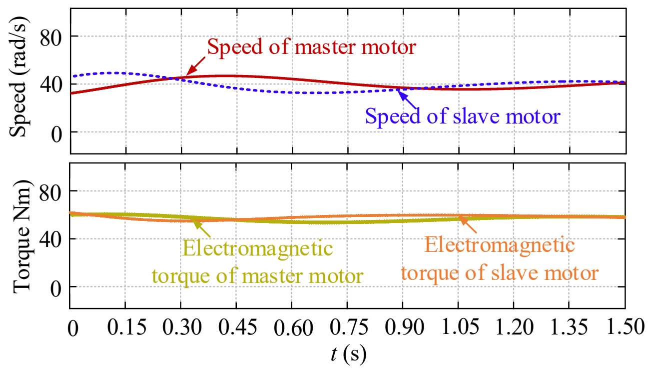

Fig. 7. Simulation results when master motor experiences load variations.

Second, after defining the PMMs connected with the tail pulley and head pulley as master motor and slave motor, respectively, a master-slave control scheme is developed. The slave motor needs to track the real-time speed of the master motor. Third, an FCS-MPSC controller is developed to improve the dynamics of the system. Meanwhile, the speed reference of the master motor incorporates the speed errors of the two motors to further improve the dynamics of the slave motor. Finally, simulation results validate the proposed coordination and FCS-MPSC methods, but also place great demand on further enhancement in coordination control.

References

[1] J. Li, G. You and S. Lei, "Fuzzy and Frequency Control System Study on Belt Conveyor," *2010 4th International Conference on Bioinformatics and Biomedical Engineering*, Chengdu, China, 2010, pp. 1-4.

[2] F. Zeng, C. Yan, Q. Wu and T. Wang, "Dynamic Behaviour of a Conveyor Belt Considering Non-Uniform Bulk Material Distribution for Speed Control," in *Applied Sciences*, vol. 10, no. 13, pp. 1-19, June 2020.

[1] C. Gan, X. Li, Z. Yu, K. Ni, S. Wang and R. Qu, "Modular Seven-Leg Switched Reluctance Motor Drive With Flexible Winding Configuration and Fault-Tolerant Capability," in *IEEE Transactions on Transportation Electrification*, vol. 9, no. 2, pp. 2711-2722, June 2023.

[3] Y. Ni and L. Chen, "Research of Energy Saving Control System of Mine Belt Conveyors," *2021 International Conference on Intelligent Transportation, Big Data & Smart City (ICITBS)*, Xi'an, China, 2021, pp. 579-581.

[4] L. Wen, B. Liang, B. Li and L. Zhang, "Power Balance Control Strategy of Permanent Magnet Synchronous Motor of Belt Conveyor," in IEEE Access, vol. 10, pp. 117045-117052, 2022.

[5] C. Gong, Y. Hu, J. Gao, Y. Wang and L. Yan, "An Improved Delay-Suppressed Sliding-Mode Observer for Sensorless Vector-Controlled PMSM," in *IEEE Transactions on Industrial Electronics*, vol. 67, no. 7, pp. 5913-5923, July 2020.

[6] J. Zhang, B. Zhang and G. Feng, "Influence of Introducing the Rotor MMF Harmonic on Torque Performance of Spoke Type Permanent Magnet Motor With FSCW," in *IEEE Access*, vol. 8, pp. 196123-196134, 2020.

[7] Q. Zhou, H. Gong, G. Du, Y. Zhang and H. He, "Distributed Permanent Magnet Direct-Drive Belt Conveyor System and Its Control Strategy," in *Energies*, vol. 15, no. 22, pp. 1-18, Nov. 2022.

[8] I. Petrov and J. Pyrhonen, "Performance of Low-Cost Permanent Magnet Material in PM Synchronous Machines," in *IEEE Transactions on Industrial Electronics*, vol. 60, no. 6, pp. 2131-2138, June 2013.

[9] T. Nagano and J. -i. Itoh, "Design of Multi-Parallel Drive Technique for System with Numbers of Permanent Magnet Synchronous Motors," *2013 IEEE 10th International Conference on Power Electronics and Drive Systems (PEDS)*, Kitakyushu, Japan, 2013, pp. 193-198.

[10] S. Zhang, J. Kang and J. Yuan, "Analysis and Suppression of Oscillation in V/F Controlled Induction Motor Drive Systems," in *IEEE Transactions on Transportation Electrification*, vol. 8, no. 2, pp. 1566-1574, June 2022.

[11] S. Rabbi, M. Little and X. Liang, "Limit Cycle Detection in Line Start Interior Permanent Magnet Motors," in *IEEE Transactions on Energy Conversion*, vol. 35, no. 3, pp. 1327-1337, Sept. 2020.

[12] H. Lv, Q. Sun, Y. Du, L. Wang and C. Li, "Electromagnetic Force Harmonics Compensation Control Strategy of Permanent Magnet Synchronous Motor Based on Multiple Proportional Resonance Controller," *2021 IEEE 4th International Electrical and Energy Conference (CIEEC)*, Wuhan, China, 2021, pp. 1-5.

[13] X. Wang, X. Zhou, W. Zhang, X. Yang, X. Zhao and B. Zhang, "Magnetic field radiation model of ultra-low frequency mechanical antenna array based on rotating permanent magnet," *2021 IEEE International Conference on Electrical Engineering and Mechatronics Technology (ICEEMT)*, Qingdao, China, 2021, pp. 562-567.

[14] Y. Han, S. Chen, C. Gong, X. Zhao, F. Zhang and Y. Li, "Accurate SM Disturbance Observer-Based Demagnetization Fault Diagnosis With Parameter Mismatch Impacts Eliminated for IPM Motors," in *IEEE Transactions on Power Electronics*, vol. 38, no. 5, pp. 5706-5710, May 2023.

[15] C. Zhang, Q. Zhang, J. He, B. Fang and J. Liu, "Total-Amount Coordinated Finite-Time Control of Multi-Motors With Saturation Constraints," in *IEEE Access*, vol. 8, pp. 221138-221147, 2020.

[16] Q. Wang and F. He, "The Synchronous Control of Multi-Motor Drive Control System with Floating Compensation," *2016 12th World Congress on Intelligent Control and Automation (WCICA)*, Guilin, China, 2016, pp. 1949-1954.

[17] Y. Zheng, H. Qu, Y. Zhao and Z. Pang, "Synchronous Control of Multi-Motor Systems Using an Improved Relative Coupling Control Structure," *2022 IEEE 11th Data Driven Control and Learning Systems Conference (DDCLS)*, Chengdu, China, 2022, pp. 1427-1432.

[18] J. Gao, C. Gong, W. Li and J. Liu, "Novel Compensation Strategy for Calculation Delay of Finite Control Set Model Predictive Current Control in PMSM," in *IEEE Transactions on Industrial Electronics*, vol. 67, no. 7, pp. 5816-5819, July 2020.

[19] S. Mariethoz, A. Domahidi and M. Morari, "High-Bandwidth Explicit Model Predictive Control of Electrical Drives," in *IEEE Transactions on Industry Applications*, vol. 48, no. 6, pp. 1980-1992, Nov.-Dec. 2012.

[20] Y. Han, C. Gong, L. Yan, H. Wen, Y. Wang and K. Shen, "Multiobjective Finite Control Set Model Predictive Control Using Novel Delay Compensation Technique for PMSM," in *IEEE Transactions on Power Electronics*, vol. 35, no. 10, pp. 11193-11204, Oct. 2020.

[21] Liu, Z. Fang, M. H. Cheung, W. Cai and J. Huang, "Mechanisms Design for Blockchain Storage Sustainability," in *IEEE Communications Magazine*, doi: 10.1109/MCOM.001.2200809.

[22] L. Ge, Z. Fan, N. Du, J. Huang, D. Xiao and S. Song, "Model Predictive Torque and Force Control for Switched Reluctance Machines based on Online Optimal Sharing Function," *IEEE Transactions on Power Electronics*, vol. 37, no. 1, pp. 1-10, Jan. 2023.

[23] Y. Zhang, L. Ding, N. Hou and Y. Li, "A Direct Actual-Power Control Scheme for Current-Fed Dual-Active-Bridge DC/DC Converter Based on Virtual Impedance Estimation," in *IEEE Transactions on Power Electronics*, vol. 37, no. 8, pp. 8963-8975, Aug. 2022.